

Origin of Entropy Convergence in Hydrophobic Hydration and Protein Folding

Shekhar Garde,^{1,2} Gerhard Hummer,¹ Angel E. García,¹ Michael E. Paulaitis,^{2,3} and Lawrence R. Pratt¹

¹Theoretical Division, Los Alamos National Laboratory, Los Alamos, New Mexico 87545

²Center for Molecular and Engineering Thermodynamics, Department of Chemical Engineering, University of Delaware, Newark, Delaware 19716

³Department of Chemical Engineering, Johns Hopkins University, Baltimore, Maryland 21218

(Received 13 September 1996)

An information theory model is used to construct a molecular explanation why hydrophobic solvation entropies measured in calorimetry of protein unfolding converge at a common temperature. The entropy convergence follows from the weak temperature dependence of occupancy fluctuations for molecular-scale volumes in water. The macroscopic expression of the contrasting entropic behavior between water and common organic solvents is the *relative* temperature insensitivity of the water isothermal compressibility. The information theory model provides a quantitative description of small molecule hydration and predicts a *negative* entropy at convergence. Interpretations of entropic contributions to protein folding should account for this result. [S0031-9007(96)01806-6]

PACS numbers: 87.15.Kg, 87.15.Da

High sensitivity calorimetry on the unfolding of globular proteins has suggested that hydrophobic contributions to the entropies of unfolding converge to zero near 385 K [1–5]. Additional thermodynamic information on protein folding processes is then obtained by extrapolating the calorimetric measurements to the convergence temperature where hydrophobic contributions vanish. The convergence behavior of entropies of solution of hydrocarbons in water is known also [6–9]. Yet a microscopic-level mechanism for this phenomenon has not been offered [10]. Here we identify a mechanism by analysis of an information theory model of hydrophobic hydration [11,12]. We show how the theory predicts entropy convergence on the basis of the density and density fluctuations of liquid water. Consistent with experimental results on hydrophobic hydration, the model predicts that the entropy at convergence should be negative.

Aqueous protein solutions are complex systems involving molecular interactions of several kinds, including those associated with ionic and polar groups, in addition to hydrophobic contributions [5]. For clarity we focus on strictly hydrophobic species and idealize those solutes as hard core objects that perfectly repel water molecule centers identified as the position of the oxygen atoms. Statistical mechanics relates the excess chemical potential of hard core solutes to the probability, p_0 , of finding an empty volume, v , or a cavity of a given size and shape in water,

$$\Delta\mu^{\text{ex}} = -kT \ln p_0. \quad (1)$$

We calculate p_0 by considering the probabilities, p_n , of observing exactly n solvent centers in the cavity. The p_n are predicted by maximizing an information entropy [11,12], subject to the constraints of available information. The experimentally accessible first and second moments of the number of solvent centers in the cavity region constitute the generally available information. This procedure yields here the distribution $p_n = \exp(\lambda_0 + \lambda_1 n + \lambda_2 n^2)$

where λ_0 , λ_1 , and λ_2 are Lagrange multipliers. The required moments are obtained from the number density ρ and oxygen-oxygen radial distribution function $g(r)$ by

$$\langle n \rangle = \rho v, \quad (2)$$

$$\langle n(n-1) \rangle = \rho^2 \int_v d\mathbf{r} \int_v d\mathbf{r}' g(|\mathbf{r} - \mathbf{r}'|). \quad (3)$$

That this is an accurate model for the circumstances considered here has been explicitly verified [11,12].

Figure 1 shows the calculated $\Delta\mu^{\text{ex}}$ for spherical solutes as a function of temperature along the saturation curve of liquid water. For comparison, chemical potentials calculated directly from simulation using test particle insertions [14] are also shown. The quantitative agreement between the two methods is excellent over the entire temperature range. The chemical potential increases with temperature past 400 K but eventually decreases. The maximum in chemical potential occurs at about the same temperature in each case. These curves have the same shape as experimental ones [16] for inert gases dissolved in water but shifted upward due to the use of a hard sphere model.

Entropies calculated as the temperature derivative of $\Delta\mu^{\text{ex}}$ along the saturation curve are shown in Fig. 2. As expected, these entropies are large and negative at room temperature, and increase with temperature. The entropies of hydration for these solutes converge in a temperature region about 400 K, close to the temperature at which they are zero. The observed entropy convergence for transfer of simple nonpolar species from the dilute gas to water [16] is similar. Since water densities and O-O radial distribution functions constitute the only input to our model, the behavior shown in Figs. 1 and 2 must arise from these properties of liquid water. We therefore examine the connection between these properties and the solvation free energies.

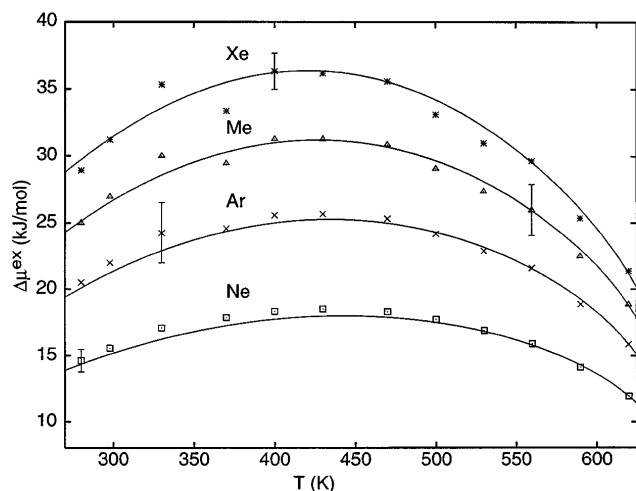


FIG. 1. Excess chemical potentials $\Delta\mu^{\text{ex}}$ of model hard sphere solutes of sizes roughly comparable to Ne, Ar, methane (Me), and Xe as a function of temperature. The hard sphere diameters used were 2.8, 3.1, 3.3, and 3.45 Å, respectively. The hard sphere diameter is then kept constant at various temperatures. The effects of more general solute-solvent interactions can be included subsequently [13]. The lines indicate the information theory model results, and the symbols are the values calculated using the test particle insertion method [14]. Typical error bars in the test particle insertion method are indicated for each solute. The required second moments were obtained from oxygen-oxygen radial distribution functions calculated from Monte Carlo simulations of 256 simple point charge (SPC) [15] water molecules.

A simplification of the two moment model gives an explicit expression connecting the chemical potential to the density and density fluctuations of liquid water,

$$\Delta\mu^{\text{ex}} \approx T\rho^2\{kv^2/2\sigma^2\} + T\{k\ln(2\pi\sigma^2)/2\}. \quad (4)$$

This is obtained from the Gaussian estimate $p_n \approx \exp(-\delta n^2/2\sigma^2)/\sqrt{2\pi\sigma^2}$ where $\delta n = n - \langle n \rangle$, and $\sigma^2 = \langle \delta n^2 \rangle$. The Gaussian formula is consistent with the Pratt-Chandler [17] theory. See Refs. [11,12,18]. Since the second term of Eq. (4) is smaller than the first and is only logarithmically sensitive to the size of the solute, this relationship says physically that the solvation free energy may be lowered by decreasing the density or the temperature of the solvent [the $T\rho^2$ factor], or by enhancing the ability of the solvent to open cavities of a size necessary to accommodate the solute [the σ^2 factor in the first term]. Along the saturation curve in Fig. 1, the combination $T\rho^2(T)$ exhibits a nonmonotonic temperature dependence. Surprisingly, $\sigma^2(T, v)$ has a negligible dependence on the temperature over that range, so that

$$\Delta\mu^{\text{ex}} \approx T\rho^2(T)x(v) + Ty(v). \quad (5)$$

The quantities $x(v)$ and $y(v)$, defined by the correspondence between Eqs. (4) and (5), depend only on the excluded volume of the solute, not on the temperature. Because the T and v dependence is important in both

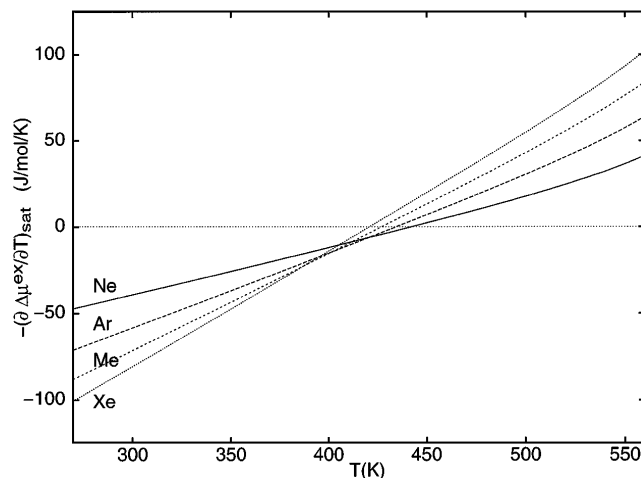


FIG. 2. $-(\partial\Delta\mu^{\text{ex}}/\partial T)_{\text{sat}}$ along the saturation curve of liquid water for model hard sphere solutes of sizes comparable to Ne, Ar, methane (Me), and Xe as a function of temperature. Note that the convergence point would be more sharply defined if the Ne results were excluded. Analysis of solubility data from different sources [16] locates the convergence temperature for Ne, Ar, methane, and Xe in the neighborhood of 400 K. This convergence region seems to move systematically to lower temperatures and entropies as data on smaller solutes are excluded, becoming more consistent with the values assumed in protein unfolding experiments. Closely examined, the width of the entropy convergence region is several times 10 K for inert gas solubilities. Additional, equation of state contributions to the standard solvation entropy are negligible: $|(\partial\mu^{\text{ex}}/\partial T)_p - (\partial\mu^{\text{ex}}/\partial T)_{\text{sat}}| < 1$ and < 10 (J/mol)/K for temperatures $T < 450$ and < 550 K, respectively.

terms of Eq. (5) we require a generalization of the arguments [6,9] based upon the hypothesis of convergence at zero entropy. Discussion of the more general argument is illustrated by the schematic Fig. 3. To begin, note [Fig. 3(a)] that if $Ty(v)$ were neglected in Eq. (5) a precise convergence at zero entropy would be observed; this follows from previous arguments [6,9]. But $Ty(v)$ is present, in fact, and adds $-k\ln(2\pi\sigma^2)/2$ to the entropies. Since this contribution varies only logarithmically with v , it provides [Fig. 3(b)] a downward shift, approximately the same for each entropy curve. An accurate convergence is obtained at the entropy $-k\ln(2\pi\sigma^2)/2$. Finally, if we include the neglected temperature dependences by obtaining the temperature derivatives of Eq. (1), the convergence is further shifted to lower temperatures and entropies and is further blurred as shown in Fig. 3(c).

In contrast, for nonpolar liquid solvents we anticipate a stronger temperature dependence for $\sigma^2(T, v)$ in addition to the nonmonotonic temperature dependence of $T\rho^2(T)$. The temperature dependences of both $T\rho^2(T)$ and $\sigma^2(T, v)$ would be needed to describe the variation of the chemical potential along the coexistence curve. Equation (5) would not apply and entropy convergence would not be expected. The macroscopic expression of this con-

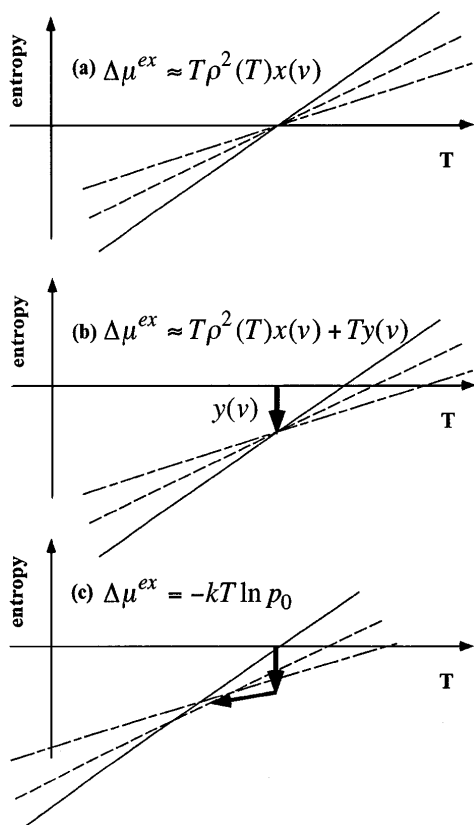


FIG. 3. $-(\partial\Delta\mu^{ex}/\partial T)_{\text{sat}}$ along the saturation curve of liquid water, as in Fig. 2 but schematically. (a) Contribution to the entropy from the $T\rho^2(T)x(v)$ term of Eq. (5). This contribution dominates Eq. (5). (b) Sum of the contributions from both the terms in Eq. (5). The constancy of $\sigma^2(T, v)$ with temperature is assumed. For the hard sphere models considered here the downward shift is about 7–9 (J/mol)/K. (c) Entropies calculated from Eq. (1) accounting for the temperature dependence of $\sigma^2(T, v)$. For the hard sphere model solutes the leftward shift is roughly 40–50 K and the curves are shifted downward by another 3–7 (J/mol)/K, approximately. The total downward shift of 10–16 (J/mol)/K is about a quarter of the entropy at room temperature; see Fig. 2.

trasting behavior is the *relative* temperature insensitivity of the water isothermal compressibility compared to hydrocarbon liquids; in comparison to benzene, normal alkanes, and carbon tetrachloride, the isothermal compressibility of liquid water varies only weakly along the saturation curve up to 450 K [19].

In conclusion, the temperature maximum in chemical potentials for hydrophobic hydration and the entropy convergence both follow directly from the weak temperature dependence of occupancy fluctuations $\sigma^2(T, v) = \langle \delta n^2 \rangle$

for solute excluded volumes in water. Further, the value of the entropy at convergence is *negative*. Interpretations of entropic contributions to protein folding should account for this result.

The excellent agreement shown in Fig. 1 between the test particle insertion results and those obtained from the information theory model demonstrates that a Gaussian distribution adequately represents molecular-scale density fluctuations in liquid water. This ability to relate physical features of water structure to the observed thermodynamics of hydrophobic hydration holds promise for extending the information theory modeling to proteins and protein-ligand complexes in aqueous solutions.

-
- [1] P. L. Privalov and N. N. Khechinashvili, *J. Mol. Biol.* **86**, 665 (1974).
 - [2] P. L. Privalov, *Adv. Protein Chem.* **33**, 167 (1979).
 - [3] P. L. Privalov and S. J. Gill, *Adv. Protein Chem.* **39**, 191 (1988).
 - [4] P. L. Privalov and G. I. Makhatadze, *J. Mol. Biol.* **232**, 660 (1993).
 - [5] G. I. Makhatadze and P. L. Privalov, *Adv. Protein Chem.* **47**, 307 (1995).
 - [6] R. L. Baldwin, *Proc. Natl. Acad. Sci. U.S.A.* **83**, 8069 (1986).
 - [7] R. L. Baldwin and N. Muller, *Proc. Natl. Acad. Sci. U.S.A.* **89**, 7110 (1992).
 - [8] L. Fu and E. Freire, *Proc. Natl. Acad. Sci. U.S.A.* **89**, 9335 (1992).
 - [9] B. Lee, *Proc. Natl. Acad. Sci. U.S.A.* **88**, 5154 (1991).
 - [10] W. Kauzmann, *Nature (London)* **325**, 763 (1987).
 - [11] G. Hummer, S. Garde, A. E. García, A. Pohorille, and L. R. Pratt, *Proc. Natl. Acad. Sci. U.S.A.* **93**, 8951 (1996).
 - [12] B. J. Berne, *Proc. Natl. Acad. Sci. U.S.A.* **93**, 8800 (1996).
 - [13] D. Chandler, J. D. Weeks, and H. C. Anderson, *Science* **220**, 787 (1983).
 - [14] L. R. Pratt and A. Pohorille, *Proc. Natl. Acad. Sci. U.S.A.* **89**, 2995 (1992).
 - [15] H. J. C. Berendsen, J. P. M. Postma, W. F. van Gunsteren, and J. Hermans, in *Intermolecular Forces: Proceedings of the 14th Jerusalem Symposium on Quantum Chemistry and Biochemistry*, edited by B. Pullman (Reidel, Dordrecht, The Netherlands, 1981), p. 331.
 - [16] A. H. Harvey, J. M. H. L. Sengers, and J. C. Tanger IV, *J. Phys. Chem.* **95**, 932 (1991).
 - [17] L. R. Pratt and D. Chandler, *J. Chem. Phys.* **67**, 3683 (1977).
 - [18] D. Chandler, *Phys. Rev. E* **48**, 2898 (1993).
 - [19] J. S. Rowlinson and F. L. Swinton, in *Liquids and Liquid Mixtures* (Butterworth Scientific, London, 1982), 3rd ed.